JPhys Materials

PAPER • OPEN ACCESS

A composition transferable and time-scale consistent coarse-grained model for cis-polyisoprene and vinyl-polybutadiene oligomeric blends

To cite this article: Takahiro Ohkuma and Kurt Kremer 2020 *J. Phys. Mater.* **3** 034007

View the article online for updates and enhancements.

You may also like

- On the microscopic foundation of dissipative particle dynamics
A. Eriksson, M. Nilsson Jacobi, J. Nyström et al.
- Sheep productivity in relation to coarse fiber in new-born lambs of different genotypes
E N Chernobai, T V Voblikova, N A Agarkova et al.
- Experimental study on particle breakage and fractal characteristics of coarse-grained soil
Du Jun and Shen Xing-gang

Recent citations

- Molecularly Informed Field Theories from Bottom-up Coarse-Graining
Nicholas Sherck *et al*
- Coarse-grained conformational surface hopping: Methodology and transferability
Joseph F. Rudzinski and Tristan Bereau

This content was downloaded from IP address 194.95.63.248 on 26/10/2021 at 12:58

IOP Publishing J. Phys. Mater. 3 (2020) 034007 https://doi.org/10.1088/2515-7639/ab906b

Journal of Physics: Materials

A composition transferable and time-scale consistent coarse-grained model for cis-polyisoprene and vinyl-polybutadiene oligomeric blends

OPEN ACCESS

RECEIVED
17 March 2020

REVISED
26 April 2020

ACCEPTED FOR PUBLICATION
5 May 2020

PUBLISHED
1 June 2020

Original Content from this work may be used under the terms of the Creative Commons Attribution 4.0 licence.

Any further distribution of this work must maintain attribution to the author(s) and the title of the work, journal citation and DOI.

Takahiro Ohkuma[1] and Kurt Kremer[2]

[1] Digital engineering division, Bridgestone corporation, 3-1-1, Ogawahigashi, Kodaira, Tokyo 187-8531, Japan
[2] Max-Planck institute for polymer research, Ackermannweg 10, 55128 Mainz, Germany

E-mail: takahiro.ohkuma@bridgestone.com and kremer@mpip-mainz.mpg.de

Keywords: coarse-graining, polymer blend, relaxation dynamics, Langevin equation

Abstract

We study a coarse-grained model for a binary blend system composed of cis-polyisoprene and vinyl-polybutadiene. Since the slow relaxation dynamics of polymers may require very long simulation times, coarse-grained descriptions are regularly used in order to reduce computational cost while keeping the essential physics. Relaxation dynamics of a coarse-grained model is sometimes accelerated by the smooth coarse-grained potentials. However, the magnitude of the acceleration may be different in different components in a multi-component system. In order to simulate a time-scale consistent dynamics, the acceleration effects should be the same across the different components. Here, we investigate a time-scale consistent coarse-grained model for a binary polymer blend. For the coarse-grained equation of motion, we adopt the Langevin equation and adjust the friction coefficients by focusing on the relaxation times of the first normal mode of the polymers. A united-atom model is used as a reference system of the coarse-graining. Since it is found that the solubility parameter of the atomistic model is much larger than the experimental result, our simulation model is not applicable for the quantitative predictions, but we utilize it as a example system to study a time scale mismatch of a coarse-grained model. We find that the coarse-grained potentials and the friction coefficients derived for one blend composition captures different compositions of the blend. Furthermore, it is found that the magnitude of the acceleration effects of the blend rarely depends on the composition ratio. This implies that our coarse-grained model can be used for inhomogeneous systems.

1. Introduction

Polymeric materials such as plastics, rubbers, and gels, are ubiquitous in our surroundings. They are soft and have long relaxation time which is compatible with the time scale of our daily life. The mechanical and rheological properties are crucially important in their practical use [1]. To understand relationships between chemical structure and the physical properties is a central subject of material design [2].

Molecular dynamics simulations have been often utilized to study the structure-property relationship. However, since relaxation modes of long polymers are widely distributed in time and can display a very long relaxation time, require a very long time to study mechanical and rheological properties in atomistic simulations. Therefore, many coarse-grained descriptions [3–14] such as bead-spring models and slip-spring models have been proposed to perform the molecular dynamics simulations. While phenomenological models can capture essential physics of the polymeric dynamics, significantefforts are often required for the parametrization to yield quantitative predictions of a real material.

In a structure-based coarse-graining method [15–18], a coarse-grained model is derived based on the chemical structure of a target material. It has been reported that several physical properties such as a stress relaxation function of polymer melts [19–21], entanglement molecular weight [19, 22], and a chemical potential of additives [23] can be quantitatively reproduced in the coarse-grained models.

According to the structure-based coarse-graining, coarse-grained potentials are derived based on a mapping rule to specify coarse-grained variables. In an iterative Boltzmann inversion method [18], the local

© 2020 The Author(s). Published by IOP Publishing Ltd

structure represented by radial distribution functions of coarse-grained beads is reproduced as a target property of the coarse-grained model. The coarse-grained potentials often accelerate the relaxation dynamics compared to the corresponding microscopic model when we simply use the potentials with the Newtonian equation of motion. A single numerical factor is often introduced to rescale the simulation time for the simplicity although the numerical factor may depend on the thermodynamic state point of the coarse-graining. It has been demonstrated that the time-recaling approach can be used to obtain a long time scale properties such as a diffusion property in homogeneous polymer melt systems [15, 17, 20, 24–29]. The acceleration effect can be advantageous for the coarse-graining from the perspective ofreducing the computational cost.

In industrial applications, polymeric materials are typically made from many ingredients by blending different polymers and nano-fillers [30]. The acceleration of relaxation dynamics of different species upon coarse-graining must be consistent in the blend systems so as to study the dynamical properties. In fact, different acceleration effects of different components have been already reported in multi-component systems of ionic liquids, lipids, polymer melts with small additives, and polymer nanocomposites [23, 24, 31–35]. For example, it is shown in [24] that in a system of polystyrene polymers with ethylbenzene molecules the acceleration factor of the ethylbenzene is smaller than that of the polystyrene beads.

Since a quantitative prediction of the time rescaling factor based on a mapping rule is not trivial, the effects on activation energies and time scale dependent scaling factors have been studied [21, 36–39]. Furthermore, applying a processing in which polymers are mixed or demixed at certain temperatures and/or under shear flows, one needs a coarse-graining model that is transferable to different temperatures, compositions, and rheological situations. Although there are some studies for polymer blends using the structure-based coarse-grained method in which the morphologies and the radial distribution functions are mainly concerned [40–45], the dynamical properties have not been well investigated. The recent progress and challenges of coarse-graining methods with consistent dynamics properties are reviewed in [46].

A natural way to resolve the time scale mismatch is to derive appropriate equations of motion for coarse-grained variables. One approach is to derive a generalized Langevin equation based on the Mori-Zwanzig projection operator method [47, 48]. The Mori-Zwanzig equation derived from a microscopic autonomous equation of motion of an isolated Hamilton system is exact and keeps the time-reversal symmetry of the system, since the dynamics of the fast variables is also involved in the equation. To close the equation of motion, with respect to the coarse-grained variables defined by the projection, some approximations and idealizations are applied to the terms of the dissipation kernel and the random forces. They may introduce a violation of the time-reversal symmetry into the coarse-grained equation of motion. For instance, a Markovian approximation is often applied by assuming a clear time scale separation between the coarse-grained variables and the degenerated degrees of freedom. Dissipative forces and random forces which reflect the degenerated degrees of freedom satisfy the fluctuation dissipation relation of second kind [49]. There are several studies on this method [50–65]. The formulation of the dissipative particle dynamics (DPD) [66, 67] is often investigated as a coarse-grained equation of motion in which the dissipation kernel depends on relative positions between two coarse-grained beads and can be evaluated from the corresponding microscopic simulations.

The issue of the time scale mismatch in multi-component systems hasrecently beenstudied in polymer solutions and in a polymer matrix with penetrant molecules [65]. Deichmann and van der Vegt showed that the diffusion properties in the polymer solutions can be well reproduced by the Mori-Zwanzig DPD-type coarse-grained equation of motion. It is also reported that, although the penetrant molecules in the coarse-grained model display slightly faster diffusion dynamics than that in the atomistic simulation, the coarse-grained model reproduces better diffusion coefficients compared to those in another coarse-grained model which is described by the Newtonian equation of motion with a Nose-Hoover thermostat.

There are also some studies in which, by assuming stochastic equation of motion for coarse-grained beads, the parameters of the equation of motion are determined through a Bayesian optimization with the corresponding microscopic trajectories [68–70]. Dissipation parameters can be also evaluated as the parameters in the assumed stochastic equation. Another example is a Markov state model based approach by defining a probability distribution of states of interest [71–73]. The thermodynamic states evolve according to a transition matrix which may include a violation of time-reversal symmetry of the dynamics, that is, a dissipation effect. The transition matrix can be derived and optimized from the corresponding microscopic trajectories.

However, deriving dissipative friction kernel usually requires extensive statistics. Several theoretical and numerical approaches has been studied for the dissipation kernel [60, 61, 74–76]. It is also not trivial to define proper states of a Markov state model in advance while keeping the transition matrix reasonably small. If the dissipation kernel is properly obtained as well as the coarse-grained potential, it is expected that the coarse-grained model recovers the original time scale as examined for velocity auto-correlation function and

diffusion coefficients in [55, 64], and then the acceleration effect of relaxation dynamics is lost. Practically, major molecular dynamics packages, such as LAMMPS [77], Gromacs [78], and ESPResSo++ [79], do not support these kinds of equation of motion such as a non-Markovian DPD equation by default or require some programming efforts.

In this study, we consider another simple approach to adjust time scales of different components. We adopt theLangevin equation [80] and attempt to adjust the friction coefficients of the coarse-grained beads. An application of the Langevin equation has been studied in [50] for liquid methanol with the multi-scale coarse-graining method [81]. They showed that the time dependence of the velocity auto-correlation function can be well reproduced if a sufficient resolution is kept in the coarse-grained model. The friction coefficients have been evaluated from the corresponding microscopic simulation.

When a friction coefficient is sufficiently large, Lanvegin dynamics undergoes an overdamped regime where the inertial degrees of freedom are degenerated as fast variables and the relaxation time can be changed by the strength of the friction coefficient [82, 83]. This approach has been studied in a water system in a context of an adaptive resolution simulation scheme to make the dynamics of the atomistic water and the coarse-grained water consistent [84]. It is demonstrated that the diffusion behavior can be adjusted by increasing the friction coefficient while keeping the static properties. Furthermore, Salerno *et al* also showed in polyethylene melts [20] that the stress relaxation time can be adjusted by varying a friction strength of the Langevin equation of motion. Although short time scale behaviors such as a velocity auto-correlation may be changed by modifying the friction coefficients, it is expected that the coarse-grained model can approximately describe slow dynamics of interests if the dynamics is well represented by the overdamped equation. The aim of this paper is to investigate the applicability of this method to a polymer blend system.

As an example, we investigate a mixture of cis-polyisoprene and atactic vinyl-polybutadiene. This is experimentally known as a miscible polymer blend [85]. The procedure to derive the coarse-grained model is divided into 3 steps. In the first step, we derive two coarse-grained models of the homopolymer melts of cis-polyisoprene and vinyl-polybutadiene, respectively. Then, we obtain two sets of coarse-grained force fields of the cis-polyisoprene and the vinyl-polybutadiene, respectively. By keeping these force fields, we derive interaction potentials between the beads of the different polymers in the second step. In the last step, we adopt the Langevin equation of motion for the polymers and adjust the friction coefficients to reproduce the ratio of the characteristic relaxation times of the two polymers. After the derivation, we also study a composition transferability of the coarse-grained model whose coarse-grained potentials and friction coefficients are fixed to those derived in a certain composition.

This manuscript is organized as follows. After introducing a united-atom model of cis-polyisoprene and vinyl-polybutadiene in section 2.1. We derive two coarse-grained models to describe the homopolymer melts of cis-polyisoprene in section 2.2.1 and of vinyl-polybutadiene in section 2.2.2, respectively. The cross interactions between the two polymers and the friction coefficients of the Langevin equation are derived referring a 50/50 blend system in the volume fractions in section 2.2.3 and section 2.3. In section 3, we examine the coarse-grained model in the different compositions, and then summarize the results in section 4.

2. Modeling

2.1. Atomistic model

Atomistic molecular dynamics simulations are performed as microscopic descriptions in this study with the united-atom models developed in [86–88] for cis-polyisoprene and in [89, 90] for atactic vinyl-polybutadiene. These united-atom models are derivatives of one united-atom model for polybutadiene [91]. The same force field parameters are assigned to the same carbon atom types. Therefore, we can naturally extend the interaction parameters to the blend systems. The force field parameters used in this study is summarized in A. The reference temperature and pressure of our simulation are chosen as 393 K ($k_{\mathrm{B}}T \sim 3.264$ kJ/mol) and 1.0 bar as a rubbery state. All molecular dynamics simulations are performed by Gromacs 5.1.4 [78].

As a homopolymer melt of cis-polyisoprene, we have prepared 512 chains composed of 24 monomers each in a periodic boundary box as studied in [19]. The initial configuration of the system is prepared from a dilute gas state and compressed by NPT simulations for around 90 ns to the target pressure. After the compression, the system is further equilibrated by a 60 ns simulation with a Nose-Hoover thermostat [92, 93] and a Parinello-Rahmann barostat [94] of the damping factors 0.5 ps and 2.0 ps, respectively, which is almost four times longer simulation than the chain end-to-end vector relaxation time. The data for coarse-graining are sampled from a 30 ns trajectory of a NVT simulation after the equilibration. The mass density and the Kuhn length at 393 K and 1.0 bar are around $\rho_m^{\mathrm{cIP}} = 0.85$ g/cm^3 and $l_K^{\mathrm{cIP}} = 0.84$ nm, respectively, which agree well with the evaluated value 0.86 g/cm^3 from an experiment [95], and 0.83 nm for polyisoprene of cis-content 93% [96]. The relaxation time of the end-to-end vectors of the chains is about 15.4 ns.

As a homopolymer melt of vinyl-polybutadiene, we have also prepared 512 chains of 24 monomers in another periodic boundary box. The system is equilibrated by the same way as done for the cis-polyisoprene melt. The density and the Kuhn length obtained by the simulation at 393 K and 1.0 bar are around ρ_m^{vBD} =0.91 g/cm^3 and l_K^{vBD} =1.4 nm. The mass density in the simulation is considerably larger than the value 0.83 g/cm^3 from experiments [97, 98]. Note that in the two experiments the vinyl content and the poly-dispersity are high and quite narrow although the molecular weight is much larger than that of the simulation. This density mismatch is also reported in a simulation [90] and presumed due to the force field parameters of the model. On the other hand, the Kuhn length is fairly in a good agreement with an experimental result 1.37 nm [96] (temperature of the experiment is not exactly the same as our case). The relaxation time of the end-to-end vectors of the chains is around 3.46 ns in our simulation. Here we use this model as a model intended to describe vinyl-polybutadiene with keeping the discrepancy of the density in mind. It is noted that any systematical modifications of the force field parameters have not been examined in this study. Since the parameters for butadiene are originally derived from the quantum chemistry calculations and experiments for the polymers whose main contents are cis and trans connection [89, 91], a modification for vinly-butadiene remains as a matter to be studied further.

Let us define the volume fraction of cis-polyisoprene in a blend of the two polymers as

$$\phi^{\mathrm{cIP}} = \frac{w^{\mathrm{cIP}}/\rho_m^{\mathrm{cIP}}}{w^{\mathrm{cIP}}/\rho_m^{\mathrm{cIP}} + w^{\mathrm{vBD}}/\rho_m^{\mathrm{vBD}}} \tag{1}$$

where w^{cIP} and w^{vBD} are the weight fraction of cis-polyisoprene and vinyl-polybutadiene in the blend, respectively. ρ_m^{cIP} and ρ_m^{vBD} are the mass densities in the cases of the homopolymer melts, respectively. The volume fraction of vinyl-polybutadiene ϕ^{vBD} is also defined by the same way and $\phi^{\mathrm{vBD}} = 1 - \phi^{\mathrm{cIP}}$.

Besides the two homopolymer melts, we consider three blend systems of different compositions, $\phi^{\mathrm{cIP}} = 0.25, 0.5$, and 0.75. A 50/50 blend system where the volume fraction $\phi^{\mathrm{cIP}} = 0.5$ contains 200 cis-polyisoprene chains and 277 vinyl-polybutadiene chains in a simulation box. A coarse-grained model is derived to reproduce the 50/50 blend system in this study. The system of $\phi^{\mathrm{cIP}} = 0.25(0.75)$ contains 67(200) chains of cis-polyisoprene and 277(92) chains of vinyl-polybutadiene, respectively. The degrees of polymerization are fixed to 24 for both polymers in the all cases.

The 50/50 blend system is also prepared from a low density gas state to a condensed state by a long NPT simulation. After this preparation, we have further performed a NPT simulation for 100 ns with the Nose-Hoover thermostat and the Parinello-Rahmann barostat for the equilibration. For coarse-graining, a 40 ns trajectory is sampled in a NVT simulation of the 50/50 blend system after the equilibration. For the other 25/75 ($\phi^{\mathrm{cIP}} = 0.25$) and 75/25 ($\phi^{\mathrm{cIP}} = 0.75$) blends, we have removed some chains from the 50/50 blend to change the volume fraction. Then, the systems are equilibrated by NPT simulations.

A blend of cis-polyisoprene and vinyl-polybutadiene is known as a miscible polymer blend in experiments [85] (references are therein). They are miscible even in high molecular weights. The solubility parameter χ evaluated by a scattering experiment [99, 100] is extremely small and negative around -8.5×10^{-4} at 393 K. In order to estimate the solubility parameter χ in our simulation model, scattering functions are calculated in the 50/50 blend. The random phase approximation in a mean-field approach for a polymer blend [101, 102] leads to a simple relationship among the scattering functions and the solubility parameter as

$$\begin{aligned} 2\chi \quad = \quad & \frac{v_0}{v_{\mathrm{cIP}}\phi^{\mathrm{cIP}}P^{\mathrm{cIP}}(q)} + \frac{v_0}{v_{\mathrm{vBD}}\phi^{\mathrm{vBD}}P^{\mathrm{vBD}}(q)} \\ & - \frac{1}{S_{\mathrm{comp}}(q)} \end{aligned} \tag{2}$$

in the incompressible limit. Here, $S_{\mathrm{comp}}(q)$ is the composition scattering function as defined below, and $P(q)$ represents the form factor of a single polymer chain in the unperturbed state. v_0 is the reference volume of the system, and v_{cIP} and v_{vBD} are the average volume of the scatters of the cis-polyisoprene and vinyl-polybutadiene, respectively.

Let us use the coarse-grained beads defined in figure 1 as the scatters of the scattering functions. The circles shown in figure 1 represent coarse-grained beads. The position of a bead is defined as the center-of-mass position of the inside atoms of the bead. The number of coarse-grained beads along the chain, N_{CG}, is 48 for both polymers in our system. We set the reference volume $v_0 = N_{\mathrm{tot}}/V$ where N_{tot} is the total number of the coarse-grained beads in the system and V is the total volume of the system. v_{cIP} and v_{vBD} can be evaluated as the average volume of the coarse-grained beads of the polymers.

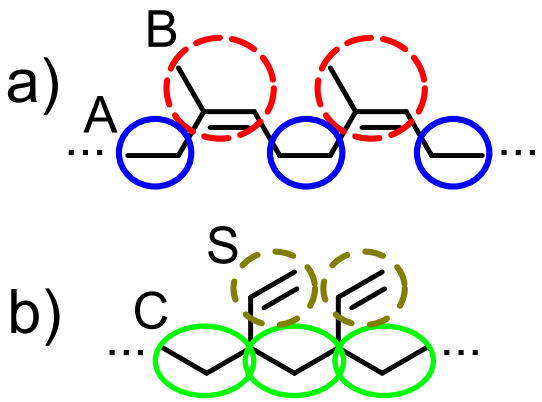

Figure 1. Mapping rules of coarse-grained beads for (a) cis-polyisoprene and (b) vinyl-polybutadiene. Two types of coarse-grained beads are defined in both polymers under the name of A, B, C, and S as indicated by circles in the figure. For the bead type C, the weight of carbons connecting to a vinyl group are equally shared by two sequent C beads.

The composition fluctuation can be defined as $\delta m(\boldsymbol{q}) = (\delta\phi_{\mathrm{cIP}}(\boldsymbol{q}) - \delta\phi_{\mathrm{vBD}}(\boldsymbol{q}))/2$ where

$$\delta\phi_{\mathrm{cIP}}(\boldsymbol{q}) = \frac{1}{\sqrt{V}}\sum_{j\in\mathrm{cIP}} v_{\mathrm{cIP}} e^{i\boldsymbol{q}\boldsymbol{R}_j},$$

$$\delta\phi_{\mathrm{vBD}}(\boldsymbol{q}) = \frac{1}{\sqrt{V}}\sum_{j\in\mathrm{vBD}} v_{\mathrm{vBD}} e^{i\boldsymbol{q}\boldsymbol{R}_j} \tag{4}$$

for $|\boldsymbol{q}| > 0$ and $\delta\phi_{\mathrm{cIP}} = \delta\phi_{\mathrm{vBD}} = 0$ at $\boldsymbol{q} = 0$. Thus, the composition scattering function $S_{\mathrm{comp}}(q)$ in the isotropic system is described as

$$\begin{aligned} S_{\mathrm{comp}}(q) &= \frac{1}{v_0}\langle \delta m(\boldsymbol{q})\delta m(-\boldsymbol{q})\rangle \\ &= \frac{1}{N_{\mathrm{tot}}}\sum_{j,k} f_j f_k \langle e^{i\boldsymbol{q}(\boldsymbol{R}_j - \boldsymbol{R}_k)}\rangle \end{aligned} \tag{5}$$

for $q > 0$ where j and k stand for all scatters. $f_j = v_{\mathrm{cIP}}/v_0$ for a scatter of cis-polyisoprene, and $f_j = -v_{\mathrm{vBD}}/v_0$ for a scatter of vinyl-polybutadiene. The ensemble average $\langle\cdot\rangle$ is evaluated by the time-average of the simulation trajectory.

In equation (2), P^{cIP} and P^{vBD} are approximately evaluated by the intra-chain scattering functions of the respective polymers in the blend. They are normalized as $P(q \to 0) = N_{\mathrm{CG}}$. Since the chains obey Gaussian statistics in a large scale that satisfies $ql_K > 1$, the form factor $P(q)$ can be described by the Debye function [101, 102].

In figure 2, the contribution from the first and second terms of the right hand side of equation (2) is plotted in red, and the third term is plotted in blue. The gyration radii in the simulation are around 1.4 nm for cis-polyisoprene and 1.1 nm for vinyl-polybutadiene. In the inset of figure 2, the whole contribution of the right hand side of equation (2) is drawn. Although it does not seem to be a constant, by averaging data of the two smallest q we obtain a rough estimate $\chi \approx 0.035$ in the scale of v_0. Thus, χN_{CG}, which is expected as a scale invariant parameter, is roughly evaluated as about 1.7 in the simulation.

As described previously, the experimentally expected χ is negative and the absolute value is extremely smaller than our simulation result. The larger bulk density of vinyl-polybutadiene in the simulation could cause the discrepancy of the miscibility of the blend. Although more larger systems are needed to evaluate more precisely the deviation of the miscibility, it is implied that the simulation model cannot quantitatively reproduce the blend properties. This indicates that our simulation model in this study should be understood as a toy model to investigate a relaxation time consistent coarse-grained model of the blend.

2.2. Coarse-grained model

2.2.1. Cis-polyisoprene melt

A coarse-grained model of the cis-polyisoprene homopolymer melt is derived in the same way as studied in [19]. We have here chosen the cut-off length of the non-bonded interactions as $r_{\mathrm{cut}} = 1.5$ nm to reduce

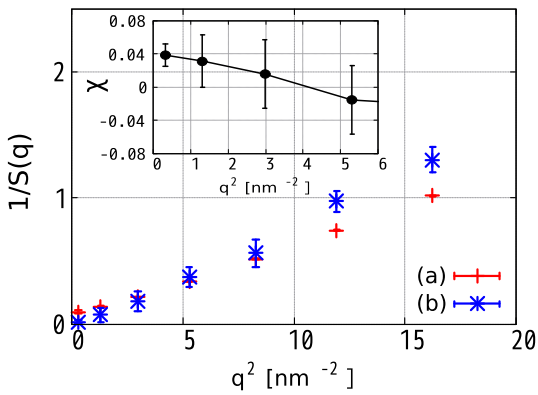

Figure 2. In the 50/50 blend system, (a) the first and second terms of the right hand side of equation (2) and (b) the third term are plotted, respectively. The coarse-grained beads represented in figure 1 are used as the scatters to compute the scattering functions. Inset, χ evaluated from equation (2) as a function of q^2 is plotted.

further the computational cost although it is 2.0 nm in [19]. Two types of coarse-grained beads A and B are defined in the monomers as illustrated in figure 1(a). The bead A contains two carbons and the bead B contains three carbons. For the bonded interactions, we define two bond potentials, two angle potentials, and two dihedral potentials. Note that since the positions of the coarse-grained beads are defined at the center-of-mass positions of the carbons inside the beads, the equilibrium bond lengths of AB and BA are different. The bonded potentials are derived through the Boltzmann inversion of the probability distribution functions of those variables obtained in the single chain simulation in vacuum [103]. We derive pressure-corrected non-bonded potentials in order to minimize the pressure difference of the blend polymers. The pressure-correction is preformed iteratively as [104]

$$V_{X,Y}^{(i+1)} = V_{X,Y}^{(i)} - A\left(1 - \frac{r}{r_{\mathrm{cut}}}\right) k_{\mathrm{B}}T, \tag{6}$$

$$A = 0.1\mathrm{sgn}(\Delta P_i)\min(1, f\Delta P_i) \tag{7}$$

with the iterative Boltzmann inversion (IBI) method [18]

$$V_{X,Y}^{(i+1)}(r) = V_{X,Y}^{(i)}(r) + \alpha_1 k_{\mathrm{B}}T \ln \frac{g_{X,Y}^{(i)}(r)}{g_{X,Y}^{(tgt)}(r)}, \tag{8}$$

where $V_{X,Y}^{(i)}$ and $V_{X,Y}^{(i+1)}$, respectively represent the ith and $(i+1)$-th candidates of the coarse-grained potential between X and Y beads, $\Delta P_i = P_i - P_{\mathrm{target}}$ is the deviation from the target pressure, and $g_{X,Y}^{(i)}$ is the radial distribution function under the potential of $V_{X,Y}^{(i)}$. The symbols X and Y represent the coarse-grained beads A or B. The pressure correction and IBI are performed alternately after the convergence of IBI steps. We have used the VOTCA package [104] for the iteration. The parameters f and α_1 are the coefficients that we can adjust to optimize the convergence of the iteration. Here, we have set empirically $f = 0.003$ so that $f\Delta P_i \approx 1$ at the first step, and $\alpha_1 = 1.0$. $g_{X,Y}^{(tgt)}$ is the target radial distribution function obtained in the atomistic simulation of the polymer melt. In figure 3, all potentials of the bonded and non-bonded interactions are shown. The distributions of the bonded variables are well reproduced as shown in figure 4(a)–(c). The agreement of the radial distribution functions with those of the atomistic simulation are also verified as shown in figure 4(d).

As studied in [19], the coarse-grained model with this mapping rule can well reproduce the Kuhn length and the linear viscoelaticity. The mean squared internal distance, $\langle R(s)^2\rangle/s$, is plotted with respect to s in figure 5(a) where $R(s)$ is the end-to-end distance of a sub-chain composed of $s+1$ beads. It is verified that not only for the end-to-end distance of the chains but bead-bead correlation in the small s region agree with those obtained from the corresponding atomistic simulation.

2.2.2. Vinyl-polybutadiene melt

A coarse-grained model of the vinyl-polybutadiene homopolymer melt is derived with the mapping rule represented in figure 1(b). The size of the coarse-grained beads are chosen to be almost the same as the beads for cis-polyisoprene. The bead C is defined from three carbons but the carbons connecting the vinyl group

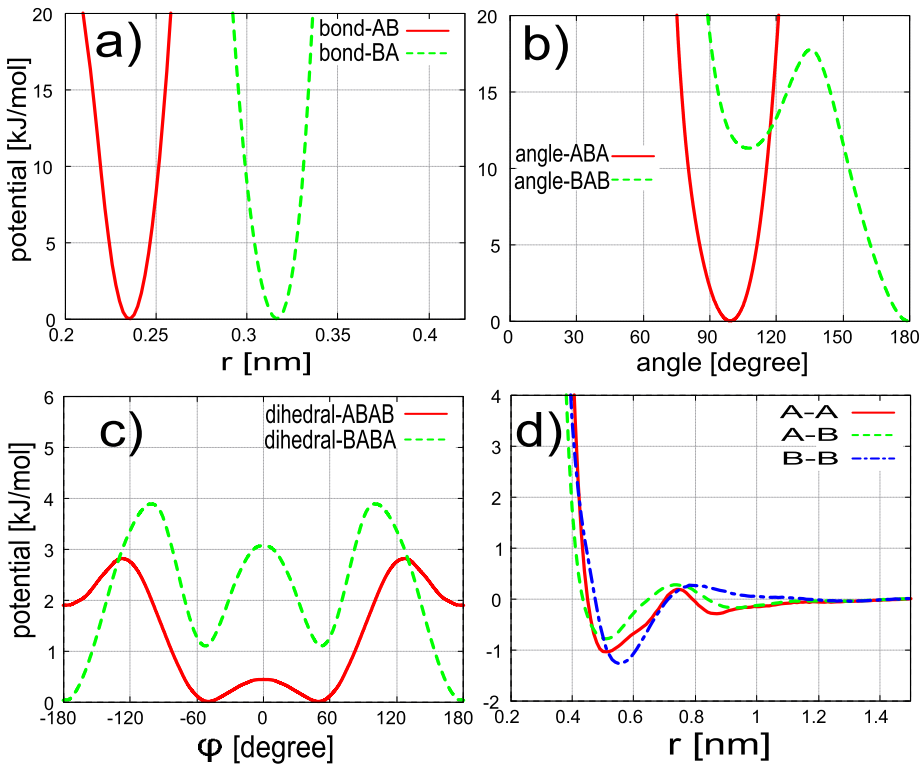

Figure 3. Coarse-grained bonded and non-bonded potentials of a cis-polyisoprene melt. Figures (a), (b), and (c) display the bond length, angle, and dihedral potentials for the coarse-grained A and B beads. The non-bonded potentials for the beads are represented in (d).

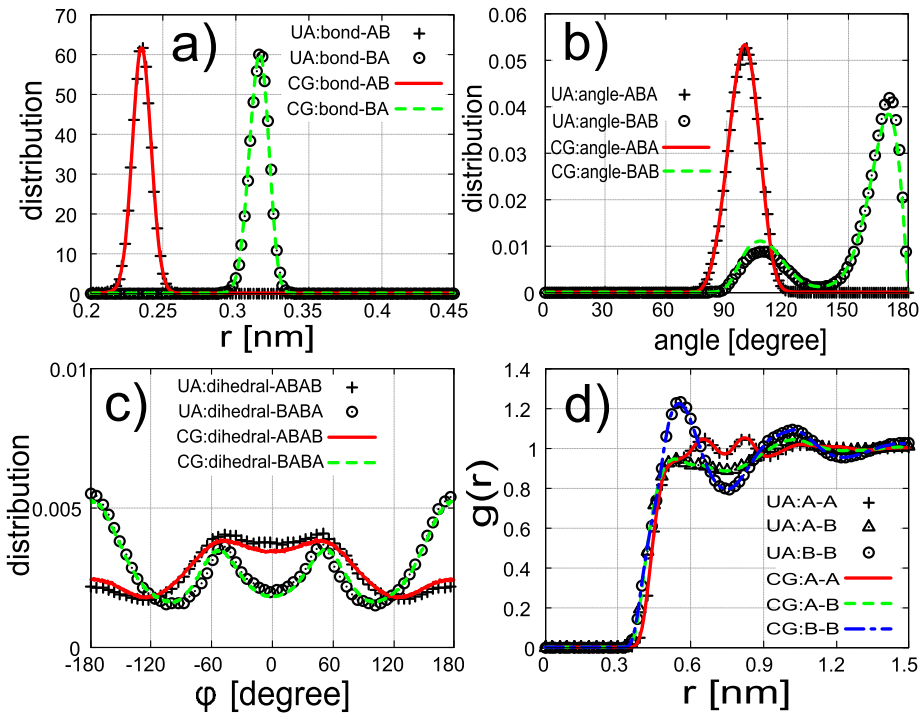

Figure 4. Distributions of the bonded variables and radial distribution functions of the coarse-grained beads of cis-polyisoprene. The results from the atomistic simulation are represented with symbols, and those from the coarse-grained model are drawn by lines. (a), (b) and (c) represent the distributions of the bond length, angles, and dihedral angles, respectively. (d) is the radial distribution functions of the beads.

are shared by the two sequent C beads in equal half weight. The beads C and S are connected alternately along the chain as studied for polystyrene in [105]. 1-5 bonded interactions between C-C and S-S along the

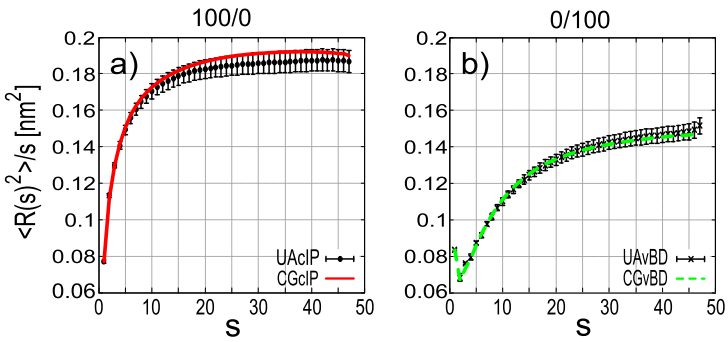

Figure 5. Mean square internal distance curves of the coarse-grained chains in the single component (a) cis-polyisoprene melt and (b) vinyl-polybutadiene melt, respectively. The results from the atomistic models are represented by symbols with error bars and those from the coarse-grained models are represented by lines.

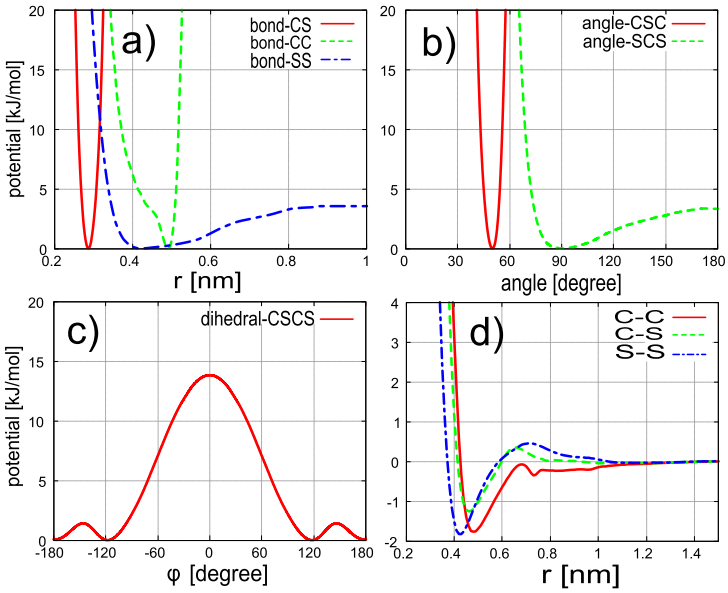

Figure 6. Coarse-grained bonded and non-bonded potentials of a vinyl-polybutadiene melt. Figures (a), (b), and (c) display the bond length, angle, and dihedral potentials for the coarse-grained C and S beads, respectively. Bond-CC and bond-SS indicate the bond length potentials between C-C and S-S of 1-5 pairs along the chain, respectively. The non-bonded potentials of the beads are represented in (d).

chain are also explicitly defined as done in [105] in order to hold the correct distance distribution between the pairs. The non-bonded interactions along the chain act from the 1-6 bonded pairs.

The bonded and non-bonded interactions are derived by the same way as for the cis-polyisoprene melt. The bonded interactions are derived by the Boltzmann inversion of the probability distribution functions obtained in the single chain simulation. The non-bonded interactions are also derived from IBI and the pressure correction as discussed for cis-polyisoprene. The resultant potentials are shown in figure 6. The distributions of the bonded variables are well reproduced as shown in figure 7(a), (b), and (c). The agreement of the radial distribution functions with those of the atomistic simulation are also verified as shown in figure 7(d).

The mean square internal distance of the coarse-grained model also agrees well with the result of the atomistic model as shown in figure 5(b). The Kuhn length of the coarse-grained model is about $l_K^{\mathrm{CGvBD}} = 1.37$ nm which agrees with $l_K^{\mathrm{vBD}} = 1.4$ nm of the atomistic model. We conclude that the two coarse-grained models for cis-polyisoprene and vinyl-polybutadiene have similar qualitiesas the representability of the polymers.

2.2.3. The 50/50 Blend

To derive the coarse-grained potentials between two polymers, let us assume that 1) the bonded interactions obtained in the single chain simulations can be used in the blend systems as well as in the homopolymer melts, and 2) we can also keep the non-bonded interactions derived in the homopolymer melts. Namely, the bonded interactions and the six non-bonded potentials between A-A, A-B, B-B, C-C, C-S, and S-S beads are

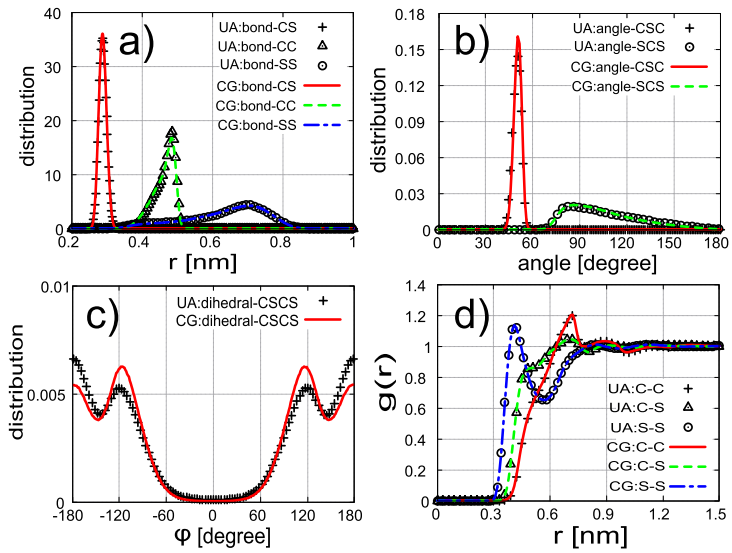

Figure 7. Distributions of the bonded variables and radial distribution functions of the coarse-grained beads of vinyl-polybutadiene. The results from the atomistic simulation are represented with symbols, and those from the coarse-grained model are represented with lines. (a), (b) and (c) represent the distributions of the bond length, angles, and dihedral angles, respectively. (d) is the radial distribution functions of the beads.

assumed to be composition transferable. Thus, we here derive the cross interactions between A-C, A-S, B-C and B-S beads in the 50/50 blend system.

To derive the cross interaction potentials, we have used IBI described in equation (8) and the coordination iterative Boltzmann inversion (C-IBI) which is described as [106]

$$V_{X,Y}^{(i+1)}(r) = V_{X,Y}^{(i)}(r) + \alpha_2 k_B T \ln \frac{C_{X,Y}^{(i)}(r)}{C_{X,Y}^{(tgt)}(r)}, \tag{9}$$

where $C_{X,Y}^{(i)}(r) = 4\pi \int_0^r dr' r'^2 g_{X,Y}^{(i)}(r')$ is the coordination number of X and Y beads. Since $C_{X,Y}^{(i)}$ is evaluated by the integration of $g_{X,Y}^{(i)}$, deviation of $g_{X,Y}^{(i)}$ at r_o is accumulated in $C_{X,Y}^{(i)}(r > r_o)$, and simultaneously deviation of $g_{X,Y}^{(i)}(r_o)$ moderately appears in $C_{X,Y}^{(i)}(r \approx r_o)$. Therefore, it is expected that IBI and C-IBI can correct the coarse-grained potentials in a different way.

We start from IBI with initial guesses of $V_{X,Y}^{(0)}(r) = [u_{X,X}(r) + u_{Y,Y}(r)]/2$ where $u_{X,X}(r)$ represents the interaction potential between X-X beads. The initial guesses are chosen because the potentials obtained by Boltzmann inversion from the target radial distribution functions cause a phase separation in the first step of IBI. Since the solubility and the radial distribution functions of the different polymer's beads are sensitive to a small difference of the interaction potentials, we have set $\alpha_1 = \alpha_2 = 0.01$ empirically. In the iteration, we have performed bathes of IBI and C-IBI alternately. In each step, 4.5 ns simulation is performed which is longer than the first normal mode relaxation time of the coarse-grained chains. During the iteration, the Nose-Hoover thermostat with a coupling factor 1.0 ps is applied to each type of the polymers. In the next subsection, we consider Langevin thermostats instead of the Nose-Hoover thermostats to study the relaxation dynamics of the polymers.

After the iteration, we obtain the coarse-grained potentials as represented in figure 8. The radial distribution functions obtained in the coarse-grained system show good agreement with those in the atomistic simulation as shown in figure 9. It is verified that the interaction potentials obtained from the homopolymer melts work well for the blend.

The mean square internal distance curves of the respective polymers are represented in figure 10. The good agreement at small s implies that the bonded potentials give accurate local configurations along the chains. For large s, the end-to-end distances of both polymers are about 7% shrink by blending in the atomistic simulation. Although the coarse-grained cis-polyisoprene reproduces the shrinkage effect, the coarse-grained vinyl-polybutadiene remains in almost the same end-to-end distance as that in the homopolymer melt. This implies that the coarse-grained model is slightly more compatible compared with the atomistic model. The composition transferability of the coarse-grained potentials is verified in section 3.

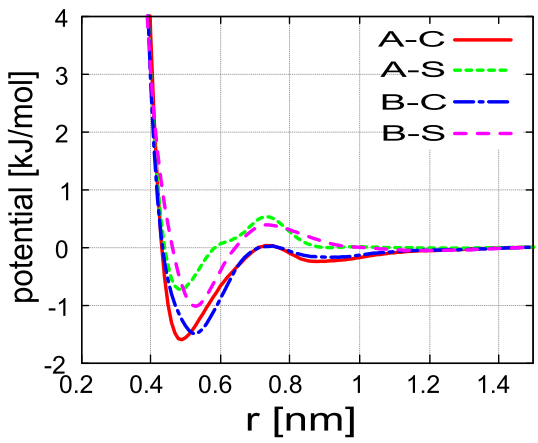

Figure 8. Coarse-grained non-bonded potentials between two beads in the different types of the polymers.

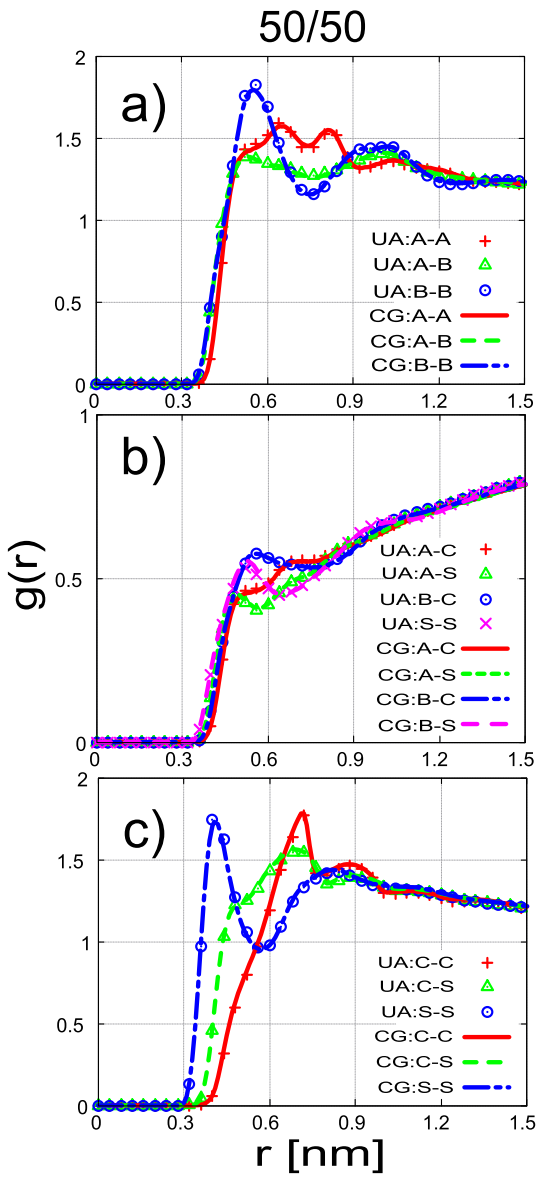

Figure 9. Radial distribution functions in the atomistic simulation are represented by symbols and those in the coarse-grained simulations are represented by lines. In (a), the radial distribution functions of beads of cis-polyisoprene are shown. In (b), those between the different polymers are shown. In (c), those of vinyl-polybutadiene are shown.

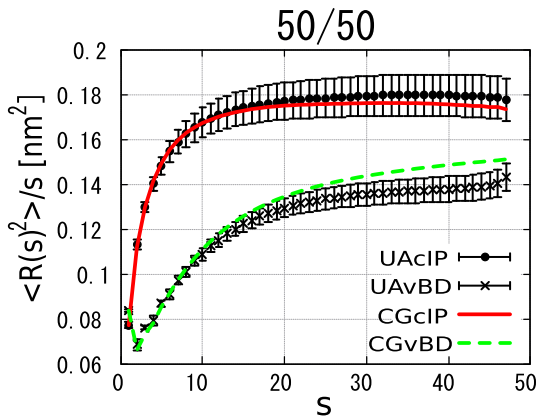

Figure 10. Mean square internal distance curves of the coarse-grained chains in the 50/50 blend are shown. The results from the atomistic models are represented by symbols with error bars and those from the coarse-grained models are represented by lines.

2.3. Relaxation times of the two polymers

As a characteristic relaxation time of the chains, we focus on the auto-correlation function of the first normal mode defined as [3]

$$C(t) = \langle \boldsymbol{X}(t)\boldsymbol{X}(0)\rangle / \langle \boldsymbol{X}(0)^2\rangle, \tag{10}$$

$$\boldsymbol{X}(t) = \sum_{j=1}^{N_{\mathrm{CG}}} \sqrt{\frac{2}{N_{\mathrm{CG}}}} \cos\left(\frac{(j-1/2)\pi}{N_{\mathrm{CG}}}\right) \boldsymbol{R}_j(t) \tag{11}$$

with the number of coarse-grained beads N_{CG} along the chain, and the coordinates of coarse-grained beads $\boldsymbol{R}_j$. The relaxation time τ_R is evaluated by fitting $C(t)$ to a single exponential function e^{-t/τ_R}. A time rescaling factor p is introduced so as to fit $C(pt)$ of the coarse-grained model to $C(t)$ of the corresponding atomistic model.

In the coarse-grained 50/50 blend with the Nose-Hoover thermostats, the two polymers show similar relaxation times of the first normal modes. The ratio of the relaxation time of cis-polyisoprene to that of vinyl-polybutadiene, $\zeta = \tau_R^{\mathrm{cIP}}/\tau_R^{\mathrm{vBD}}$, is obtained as approximately 1.3 although the ratio in the atomistic simulation is ~ 2.8. The relaxation times of the coarse-grained polymers weakly depend on the damping factors of the thermostats. This discrepancy results from the different magnitude of the time scale acceleration effect of the two polymers.

Therefore, the ratio of the relaxation times of the two polymers needs to be corrected keeping as large an acceleration of the coarse-grained model as much as possible. Since cis-polyisoprene displays too fast relaxation compared to vinyl-polybutadiene, we attempt to make cis-polyisoprene slower while keeping the relaxation dynamics of vinyl-polybutadiene as fast as possible. To perform this, we consider a simple Langevin equation described as

$$m\frac{d^2}{dt^2}R_j = -m\gamma\frac{d}{dt}R_j - \frac{\partial U}{\partial R_j} + \xi_j(t). \tag{12}$$

for the coarse-grained beads R_j with the mass m, a friction coefficient γ, and Gaussian white noise $\xi_j(t)$ which satisfies the fluctuation dissipation relation

$$\langle \xi_j(t)\xi_k(t')\rangle = 2\,\mathrm{m}\gamma k_{\mathrm{B}} T\delta_{jk}\delta(t-t'). \tag{13}$$

U represents the total interaction energy of the coarse-grained model. If the friction coefficient is sufficiently large, the relaxation time is inversely proportional to γ. The values of m, γ, and then ξ may depend on the types of the coarse-grained beads. As the friction coefficients, we use the same value of γ^{CGcIP} for the two bead types of the cis-polyisoprene and the same value of γ^{CGvBD} for the two bead types of the vinyl-polybutadiene.

Since the friction coefficient does not change the equilibrium distribution because of the fluctuation dissipation relation, it can be used to vary the relaxation time while keeping the static properties unchanged. We first fix the friction coefficient of the beads of vinyl-polybutadiene, γ^{CGvBD}, to be sufficiently small. Then, we increase γ^{CGcIP} which is the friction coefficient of the beads of cis-polyisoprene until the ratio becomes

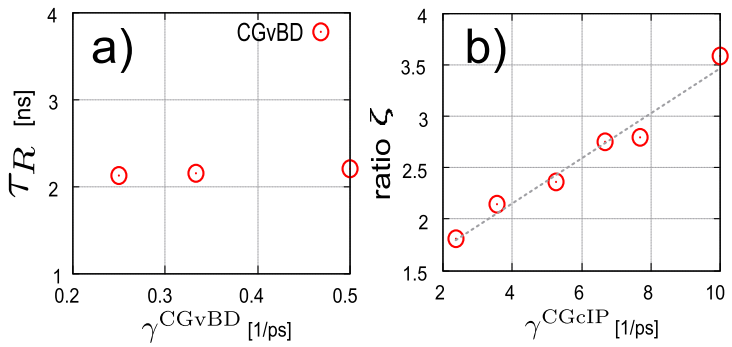

Figure 11. Dependency of the friction coefficients on the relaxation times. In (a), the first normal mode relaxation time of vinyl-polybutadiene is represented with respect to the friction coefficient for C and S beads. The ratio of the relaxation times, ζ, is plotted against the friction coefficient for A and B beads where γ^{CGvBD} is fixed to 0.5 ps^{-1}. The dash lines is an eye guide.

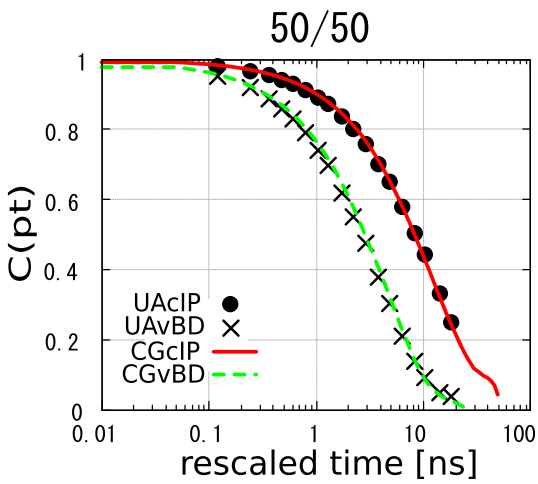

Figure 12. Relaxation behavior of the normalized auto-correlation function $C(pt)$. The results obtained in the atomistic simulation are represented by symbols, and those in the coarse-grained model are represented by lines. $p = 1.7$ is used as the time rescaling factor of the coarse-grained model.

the target value $\zeta = \tau_R^{\mathrm{CGcIP}}/\tau_R^{\mathrm{CGvBD}} \approx 2.8$ where τ_R^{CGcIP} and τ_R^{CGvBD} mean the relaxation time of the first normal modes of the coarse-grained cis-polyisoprene and vinyl-polybutadiene, respectively.

In the Langevin simulations, we find that $\gamma^{\mathrm{CGvBD}} = 0.5$ ps^{-1} is small enough as shown in figure 11(a) and smaller than the intrinsic segmental friction of the chains as confirmed below. While keeping the value of γ^{CGvBD}, we vary γ^{CGcIP}. The ratio of the relaxation times is represented in figure 11(b) with respect to γ^{CGcIP}. With approaching the overdamped regime, the relaxation time of cis-polyisoprene is increased and the target ratio is reproduced around $\gamma^{\mathrm{CGcIP}} = 6.67$ ps^{-1}. As shown in figure 12, the auto-correlation functions of the first normal modes in the coarse-grained model with $\gamma^{\mathrm{CGvBD}} = 0.5$ ps^{-1} and $\gamma^{\mathrm{CGcIP}} = 6.67$ ps^{-1} agree well with those of the atomistic simulation where we have used a single time rescaling factor $p = 1.7$ for both polymers.

It should be noted that the damping time of inertia with the Langevin thermostat is typically estimated as the order of γ^{-1}. Therefore, changing the value of γ may change the relaxation dynamics in this short time scale. According to the renormalization group method [107], by expanding the underdamped equation described as equation (12) in the limit of $\gamma^{-1} \to 0$, the overdamped equation described as

$$m\gamma \frac{d}{dt} R_j = -\frac{\partial U}{\partial R_j} + \xi_j(t) \tag{14}$$

can be derived theoretically. Therefore, when dynamics of interests changes in a much longer time scale than γ^{-1}, the overdamped picture becomes a good approximation although we cannot expect that the overdamped coarse-grained model well reproduce the short time behaviors around γ^{-1}. In the overdamped Langevin equation, the friction coefficient controls the time scale as equation (14) is invariant under the transformation of $t \to t' = pt$ and $\gamma \to \gamma' = p\gamma$ where p is a constant and independent of j. We adjust the balance of γ^{CGcIP} and γ^{CGvBD} in the overdamped picture.

Table 1. Several characteristic parameters of the polymers in the 50/50 blend. N_K, l_K, and m_K represent the number of segment along the chain, the Kuhn length, and the segmental mass. τ_R and τ_s represent the longest Rouse relaxation time of the chains and its segmental relaxation time evaluated from equation (15). The segmental friction divided by the segmental mass is represented as ς/m_K.

	united-atom		coarse-grained	
parameter	cIP	vBD	cIP	vBD
N_K	14	3.7	14	3.6
l_K (nm)	0.77	1.3	0.76	1.4
m_K (g/mol)	117	374	115	391
τ_R (ns)	12.0	4.34	7.15	2.51
τ_s (ps)	62	320	35	200
ς/m_K (ps^{-1})	85	44	52	25

To confirm the segmental relaxation time τ_s as a basic time scale of the chain dynamics and the effective segmental friction coefficient ς/m_K where m_K is the mass of a segment. We apply the Rouse model [108], which is a bead-spring model of a single ideal chain in a medium, in the blend system as an approximation. The Rouse relaxation time of the first normal mode is described with the segmental friction ς, the Kuhn length l_K, and the number of Kuhn segments N_K along the chain as

$$\tau_R = \tau_s N_K^2 = \frac{\varsigma N_K^2 l_K^2}{3\pi^2 k_B T}. \tag{15}$$

As summarized in table 1, for both types of the polymers that the segmental relaxation time is much larger than the effective damping time m_K/ς of the segment. This implies that the polymeric relaxation dynamics can be well described in the overdamped picture in which the potential interactions play an important role compared with the inertial relaxation.

3. Composition transferability

As a verification of composition transferability of the coarse-grained model, we consider the blends of $\phi^{\mathrm{cIP}} = 0, 0.25, 0.75$, and 1.0. $\phi^{\mathrm{cIP}} = 0$ and 1.0 corresponds to the single homopolymer melts of vinyl-polybutadiene and cis-polyisoprene, respectively. The coarse-grained potentials and the friction coefficients derived in the 50/50 blend system are used for the simulations of the different compositions.

As the static properties, the radial distribution functions and the mean square internal distance curves are represented in figure 13 and figure 14. The systems $\phi^{\mathrm{cIP}} = 0$ and 1.0 are omitted because they are the same as shown in figures. 4, 5, and 7. Although the beads of the minor component are slightly more structured in the atomistic model compared with the coarse-grained model, the coarse-grained model captures quite well the changes of the radial distribution functions. Moreover, the tendency of the weak shrinkage in the end-to-end distance caused of the minor component is also well reproduced as seen in figure 14.

For the relaxation dynamics, we verify the ratio of the relaxation times as well as the time rescaling factor. The auto-correlation functions of the first normal modes excellently agree with the results of the atomistic simulation as shown in figure 15. The time rescaling factor p is evaluated in each composition by comparing results from the atomistic model and the coarse-grained model. Although p in the pure vinyl-polybutadiene system is around 20 % larger than the others, it is found that p does not much depend on composition.

In figure 16, the relaxation times of the two polymers with respect to the blend composition are represented where $p = 1.7$ is used in the all cases of the coarse-grained simulations. The agreement in figure 16 implies that the change of the relaxation times are mainly caused by the interaction potentials and the effect of the friction coefficients are minor compared with the composition difference in the present model.

4. Summary

We have derived a coarse-grained model of the oligomeric polymer blend of cis-polyisoprene and vinyl-polybutadiene based on a united-atom model. Since the atomistic model of the blends studied shows considerably less miscibility compared with the experimental results, it is considered as a model system to study a time-scale consistent coarse-grained model. The discrepancy presumably comes from the force field parameters for vinyl-polybutadiene because the homopolymer melt displays a higher mass density in the simulation compared to the experimental result.

The non-bonded interaction potentials between the coarse-grained beads of the different polymers are derived in the 50/50 blend system while keeping the bonded and the non-bonded interactions of the beads within the identical polymers which are derived in their homopolymer melt systems. As characteristic

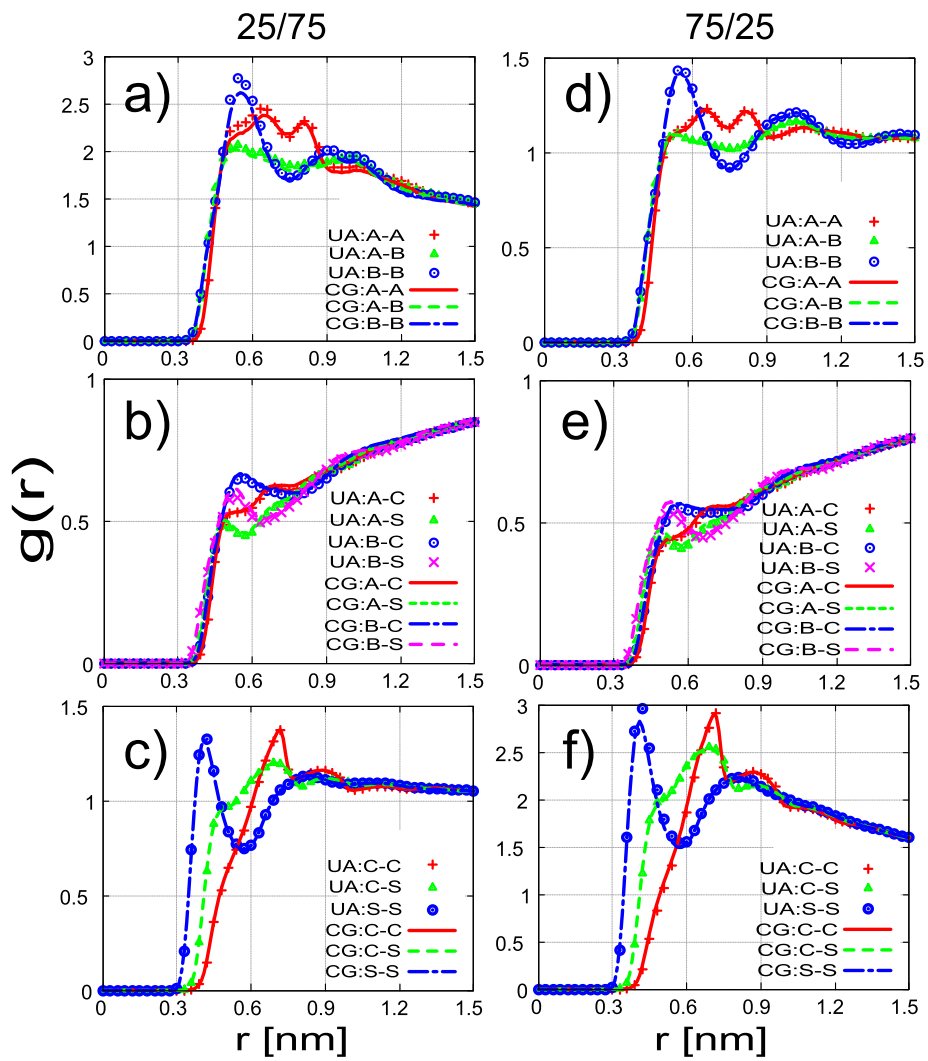

Figure 13. Radial distribution functions of the atomistic simulation are represented by symbols and those in the coarse-grained simulations are represented by lines. Figures (a), (b), and (c) show the results of the blend of cIP/vBD= 25/75 in volume fraction, and figures (d), (e), and (f) show the results of the cIP/vBD= 75/25 blend in volume fraction, respectively. In (a) and (d), the radial distribution functions of cis-polyisoprene are shown. In (b) and (e), those between the beads of the different polymers are shown. In (c) and (f), those of vinyl-polybutadiene are shown.

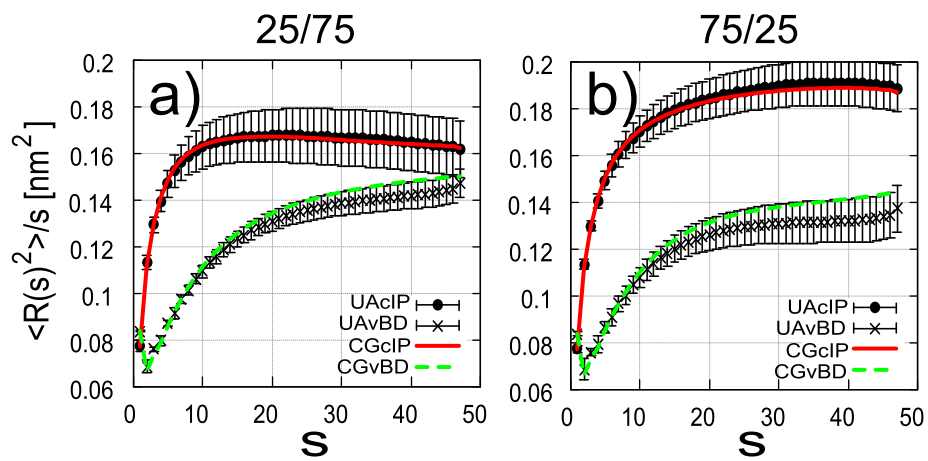

Figure 14. Mean square internal distance curves of the coarse-grained chains in the (a) 25/75 and (b) 75/25 blends results from the atomistic models are represented by symbols with error bars and those from the coarse-grained models are represented by lines.

relaxation dynamics, the first normal modes of the polymers are concerned. The ratio of the relaxation times of the two polymers are corrected by adjusting the friction coefficients of the Langevin equation for the

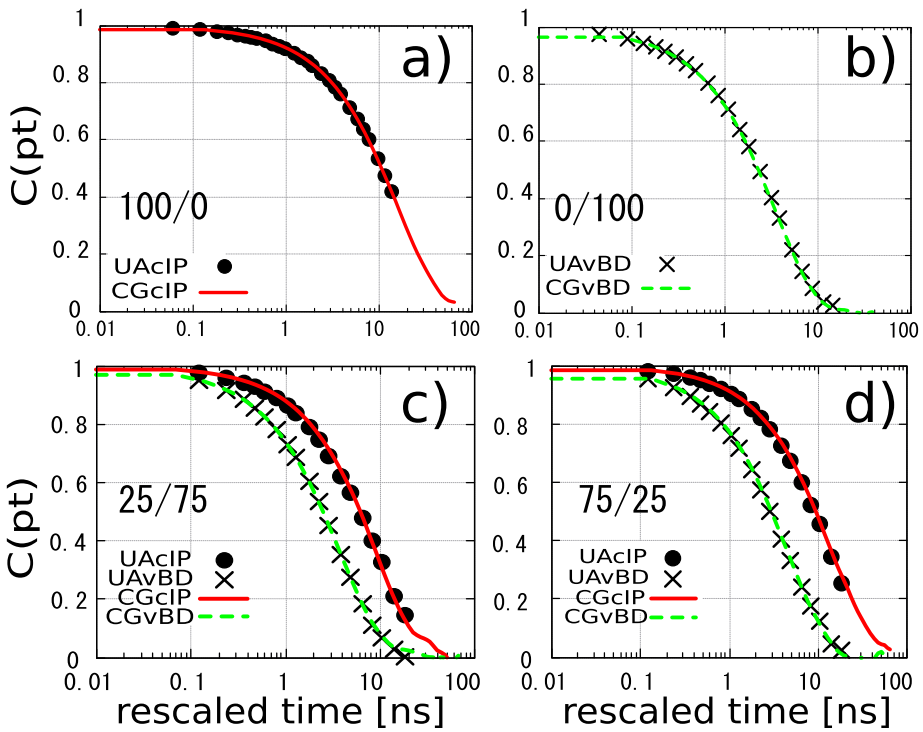

Figure 15. Relaxation behavior of the normalized auto-correlation function $C(pt)$ for (a) the pure cis-polyisoprene melt, (b) the pure vinyl-polybutadiene melt, (c) the cIP/vBD= 25/75 blend, and (d) the cIP/vBD= 75/25 blend, respectively. The results obtained in the atomistic simulation are represented by symbols and those in the coarse-grained model are represented by lines. The time rescaling factor p is set as 1.7, 1.6, 1.7, and 2.0 for cIP/vBD= 100/0, 75/25, 25/75, and 0/100, respectively.

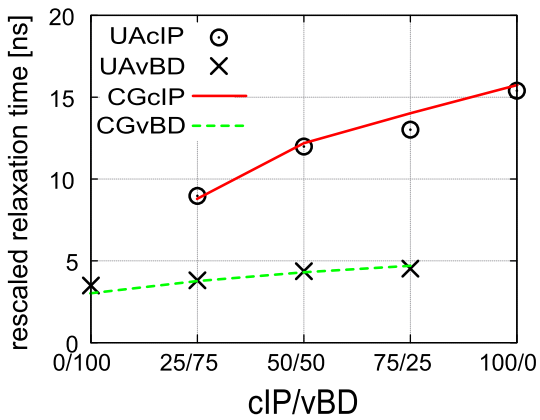

Figure 16. Relaxation times of the first normal modes of cis-polyisoprene and vinyl-polybutadiene in the blends, respectively. The x-axis shows the blend composition in the volume fraction. The relaxation times obtained by the coarse-grained model are rescaled by a single factor $p = 1.7$ in the all cases.

coarse-grained beads. It is found that the present coarse-grained model reproduces very well the radial distribution functions of the systems for different blend compositions. In addition to the static property, the ratios of the relaxation times of the two polymers are also well reproduced by the coarse-grained model derived in the 50/50 blend. Moreover, it is also found that the time rescaling factors of the different blend compositions are almost the same although they deviate maximally around 20 %.

The adjusted friction coefficients in the Langevin equation are smaller than the effective segmental friction coefficients evaluated based on the Rouse model, respectively. Although the short time scale behaviors such as the inertial relaxation may be changed by the modification of the friction coefficients, it is confirmed that the segmental relaxation time is much longer than the damping time of the segmental friction in the Rouse picture. Therefore, in the coarse-grained model, it is expected that Rouse-like dynamics is well described by the overdamped equation of motion where the potential interactions play an essential role.

Table A1. Bonded parameters of the united-atom force field are shown. The units of the lengths and energies are set to nm and kJ/mol. The angles are written in degree.

bond length	r_b					
CH2, CH2b	0.153					
CH2b, C =	0.150					
C = , CH =	0.134					
CH = , CH2	0.150					
C = , CH3	0.150					
CH2, CH	0.153					
CH, CH =	0.150					
CH = , CH2 =	0.134					
angle	k_θ	θ_0				
CH2b, C = , CH =	374.00	125.90				
CH3, C = , CH =	374.00	125.90				
C = , CH = , CH2	374.00	125.90				
CH = , CH2, CH2b	481.160	111.65				
CH2, CH2b, C =	481.160	111.65				
CH2, CH, CH2	481.167	111.65				
CH, CH2, CH	519.570	114.0				
CH2, CH, CH =	481.167	116.65				
CH, CH = , CH2 =	374.00	125.90				
proper dihedral	c_0	c_1	c_2	c_3	c_4	c_5
CH2b, C = , CH = , CH2	-14.036	20.662	1.410	-23.314	1.188	-8.400
C = , CH = , CH2, CH2b	4.603	-1.509	2.835	-6.174	-2.666	12.70
CH2, CH2b, C = , CH =	4.603	-1.509	2.835	-6.174	-2.666	12.70
CH2, CH, CH2, CH	-15.437 8	7.545	-0.30 714	-13.936 5	4.705 1	-4.05 469
CH2, CH, CH = , CH2 =	1.44 385	-6.73 845	-5.52 731	1.68 541	2.51 631	3.67 011
improper dihedral	k_ϕ	ϕ_0				
CH2b, C = , CH = , CH2	160.00	0.000				
CH, C = , CH = , CH2	160.00	180.0				

The composition transferability implies that the coarse-grained model can be applicable in inhomogeneous states such as a mixing process at least near equilibrium conditions when hydrodynamic interactions are not important. To what extent the coarse-grained model works far from equilibrium states still has to be tested because all coarse-grained parameters are derived and verified in the equilibrium state. It should be also noted that the coarse-grained potentials and the friction coefficients depend on the thermodynamics state point in which they are derived. Further studies are necessary to obtain thermodynamics transferability such as temperature transferability.

The examinations in the systems of different molecular weights and different solubility situations are also left for the future studies. In general, a polymer blend undergoes phase separation when χ is positive and molecular weights of the polymers are sufficiently large. If the coarse-grained potentials are transferable not only for composition but for molecular weight, it is expected that the coarse-grained model can capture morphological differences by the blend composition. To verify static and dynamical properties of the coarse-grained model, interfacial energy and composition fluctuation dynamics near phase boundaries also need to be investigated. Since the method to derive the time scale consistent model studied here is not specific for the polymers, it can be examined for other blend systems.

Appendix A. Parameters of the united-atom model

The force filed parameters for cis-polyisoprene and vinyl-butadiene are taken from the literatures [86–90]. The parameter used in our simulations is summarized in table A1 for the bonded parameters and in table A2 for the non-bonded parameters. The corresponding symbols of the united carbons atoms are shown in figure A1. The bond lengths are fixed by LINCS algorithm. Harmonic functions described as $(1/2)k_\theta(\theta-\theta_0)^2$ are used for the angluar potentials. For the proper and improper dihedral angles, Ryckaert-Bellemans function described as $\sum_{n=0}^{5}(-1)^n c_n \cos^n\phi$ and a harmonic function as $(1/2)k_\phi(\phi-\phi_0)^2$ are used, respectively.

Table A2. Non-bonded parameters of the united-atom force field used in our simulations are shown. The units of the lengths and energies are set to nm and kJ/mol.

non-bonded	σ	ε
C =, C =	0.33 854	0.418 400
C =, CH =	0.33 854	0.418 400
C =, CH2 =	0.33 854	0.418 400
C =, CH	0.33 854	0.418 400
C =, CH2	0.37 926	0.424 676
C =, CH2b	0.37 926	0.424 676
C =, CH3	0.37 926	0.629 692
CH =, CH =	0.33 854	0.418 400
CH =, CH2 =	0.33 854	0.418 400
CH =, CH	0.33 854	0.418 400
CH =, CH2	0.37 926	0.424 676
CH =, CH2b	0.37 926	0.424 676
CH =, CH3	0.37 926	0.629 692
CH2 =, CH2 =	0.33 854	0.418 400
CH2 =, CH	0.33 854	0.418 400
CH2 =, CH2	0.37 926	0.424 676
CH2 =, CH2b	0.37 926	0.424 676
CH2 =, CH3	0.37 926	0.629 692
CH, CH	0.33 854	0.418 400
CH, CH2	0.37 926	0.424 676
CH, CH2b	0.37 926	0.424 676
CH, CH3	0.37 926	0.629 692
CH2, CH2	0.40 090	0.391 622
CH2, CH2b	0.40 090	0.391 622
CH2, CH3	0.40 090	0.609 190
CH2b, CH2b	0.40 090	0.391 622
CH2b, CH3	0.40 090	0.030 4 595
CH3, CH3	0.40 090	0.947 2 576

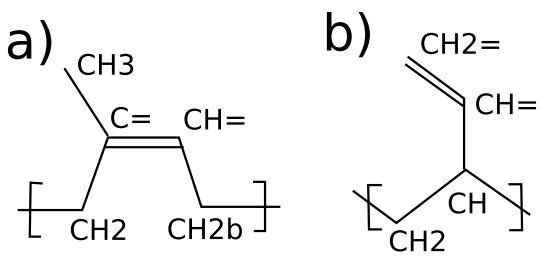

Figure A1. The repeated units of cis-polyisoprene and vinyl-polybutadiene are represented in (a) and (b), respectively. The atom names are labeled to the corresponding carbons.

Lennard-Jones potentials described as $4\epsilon[(\sigma/r)^{12} - (\sigma/r)^{6}]$ with a cut-off length 1.1 nm are assumed for the non-bond interactions in the simulation.

ORCID iD

Takahiro Ohkuma https://orcid.org/0000-0002-1629-8433

References

[1] Larson R G 1998 *The Structure and Rheology of Complex Fluids* (Oxford: Oxford Univ Press)
[2] Jancar J, Douglas J F, Starr F W, Kumar S K, Cassagnau P, Lesser A J, Sternstein S S and Buehler M J 2010 Current issues in research on structure-property relationships in polymer nanocomposites *Polymer* **51** 3321
[3] Kremer K and Grest G S 1990 Dynamics of entangled linear polymer melts: A moleculardynamics simulation *J. Chem. Phys.* **92** 5057
[4] Vettorel T, Besold G and Kremer K 2010 Fluctuating soft-sphere approach to coarse-graining of polymer models *Soft Matter* **6** 2282
[5] Murat M and Kremer K 1998 From many monomers to many polymers: Soft ellipsoid model for polymer melts and mixtures *J. Chem. Phys.* **108** 4340

[6] Masubuchi Y, Takimoto J, Koyama K, Ianniruberto G, Marrucci G and Greco F 2001 Brownian simulations of a network of reptating primitive chains *J. Chem. Phys.* **115** 4387
[7] Doi M and Takimoto J 2003 Molecular modeling of entanglement *Phil. Trans. Royal Soc. London Ser.* A **361** 641
[8] Likhtman A E 2005 Single-chain slip-link model of entangled polymers: Simultaneous description of neutron spin-echo, rheology and diffusion *Macromolecules* **38** 6128
[9] Tzoumanekas C and Theodorou D N 2006 From atomistic simulations to slip-link models of entangled polymer melts: Hierarchical strategies for the prediction of rheological properties *Curr. Opin. Solid State Mater. Sci.* **10** 61
[10] Schieber J D and Andreev M 2014 Entangled polymer dynamics in equilibrium and flow modeled through slip links *Ann. Rev. Chem. Biomol. Eng.* **5** 367
[11] Uneyama T and Masubuchi Y 2012 Multi-chain slip-spring model for entangled polymer dynamics *J. Chem. Phys.* **137** 154902
[12] Sirk T W, Slizoberg Y R, Brennan J K, Lisal M and Andzelm J W 2012 An enhanced entangled polymer model for dissipative particle dynamics *J. Chem. Phys.* **136** 134903
[13] Langeloth M, Masubuchi Y, Böhm M C and Müller-Plathe F 2013 Recovering the reptation dynamics of polymer melts in dissipative particle dynamics simulations via slip-springs *J. Chem. Phys.* **138** 104907
[14] Sgouros A P, Megariotis G and Theodorou D N 2017 Slip-spring model for the linear and nonlinear viscoelastic properties of molten polyethylene derived from atomistic simulations *Macromolecules* **50** 4524
[15] Tschöp W, Kremer K, Batoulis J, Bürger T and Hahn O 1998 Simulation of polymer melts. i. coarse-graining procedure for polycarbonates *Acta Polymer* **49** 61
[16] Tschöp W, Kremer K, Hahn O, Batoulis J and Bürger T 1998 Simulation of polymer melts. ii. from coarse-grained models back to atomistic description *Acta Polymer* **49** 75
[17] Peter C and Kremer K 2009 Multiscale simulation of soft matter systems - from the atomistic to the coarse-grained level and back *Soft Matter* **5** 4357
[18] Müller-Plathe F 2002 Coarse-graining in polymer simulation: from the atomistic to the mesoscopic scale and back *Chem. Phys. Chem.* **3** 754
[19] Ohkuma T and Kremer K 2017 Comparison of two coarse-grained models of cis-polyisoprene with and without pressure correction *Polymer* **130** 88
[20] Michael Salerno K, Anupriya A, Peters B L, Perahia D and Grest G S 2016 Dynamics in entangled polyethlene melts *Eur. Phys. J. Spec. Top.* **225** 1707
[21] Agrawal V, Holzworth K, Nantasetphong W, Amirkhizi A V, Oswald J and Nemat-Nasser S 2016 Prediction of viscoelastic properties with coarse-grained molecular dynamics and experimental validation for a benchmark polyurea system *J. Polymer Sci. B: Polymer Phys.* **54** 797
[22] Li Y, Kröger M and Liu W-K 2011 Primitive chain network study on uncrosslinked and crosslinked cis-polyisoprene polymers *Polymer* **52** 5867
[23] Dominik F, Herbers C R, Kremer K and van der Vegt N F A 2009 Hierarchical modeling of polymer permeation *Soft Matter* **5** 4556
[24] Fritz D, Konstantin K, Harmandaris V A, van der Vegt N F A and Kremer K 2011 Multiscale modeling of soft matter: scaling of dynamics *Phys. Chem. Chem. Phys.* **13** 10412
[25] Padding J T and Briels W J 2011 Systematic coarse-graining of the dynamics of entangled polymer melts: The road from chemistry to rheology *J. Phys. Cond. Matt.* **23** 233101
[26] Michael Salerno K, Agrawal A, Perahia D and Grest G S 2016 Resolving dynamic properties of polymers through coarse-grained computational studies *Phys. Rev. Lett.* **116** 058302
[27] Peters B L, Michael Salerno K, Ting G, Perahia D and Grest G S 2018 Effect of chain length dispersity on the mobility of entangled polymers *Phys. Rev. Lett.* **121** 057802
[28] Karimi-Varzaneh H A, van der Vegt N F A, Müller-Plathe F and Carbone P 2012 How good are coarse-grained polymer models? a comparison for atactic polystyrene *ChemPhysCem* **13** 3428
[29] Choudhury C K, Carbone P and Roy S 2016 Scalability of coarse-grained potentials generated from iterative boltzmann inversion for polymers: Case study on polycarbonates *Macromol. Theory Simul.* **25** 274
[30] Dick J S 2014 *How to Improve Rubber Compounds* (Cincinnati, OH: Hanser)
[31] Marrink S J, de Vries A H and Mark A E 2004 Coarse grained model for semiquantitative lipid simulations *J. Phys. Chem.* B **108** 750
[32] Thøgersen L, Schiøtt B, Vosegaard T, Niels C N and Tajkhorshid E 2008 Peptide aggregation and pore formation in a lipid bilayer: A combined coarse-grained and all atom molecular dynamics study *Biophys. J.* **95** 4337
[33] Karimi-Varzaneh H A, Müller-Plathe F, Balasubramanian S and Carbone P 2010 Studying long-time dynamics of imidazolium-based ionic liquids with a systematically coarse-grained model *Phys. Chem. Chem. Phys.* **12** 4714
[34] Wang Y-L, Lyubartsev A, Zhong-Yuan L and Laaksonen A 2013 Multiscale coarse-grained simulations of ionic liquids: comparison of three approaches to derive effective potentials *Phys. Chem. Chem. Phys.* **15** 7701
[35] Smith G D, Bedrow D, Liwei Li and Byutner O 2002 A molecular dynamics simulation study of the viscoelastic properties of polymer nanocomposites *J. Chem. Phys.* **117** 9478
[36] Depa P K and Maranas J K 2005 Speed up of dynamic observables in coarse-grained molecular-dynamics simulations of unentangled polymers *J. Chem. Phys.* **123** 094901
[37] Depa P K and Maranas J K 2007 Dynamic evolution in coarse-grained molecular dynamics simulations of polyethylene melts *J. Chem. Phys.* **126** 054903
[38] Meinel M K and Florian M-P 2020 Loss of molecular roughness upon coarse-graining predicts the artificially accelerated mobility of coarse-grained molecular simulation models *J. Chem. Theory Comput.* **16** 1411
[39] Song J, Hsu D D, Shull K R, Phelan Jr. F R, Douglas J F, Xia W and Keten S 2018 Energy renormalization method for the coarse-graining of polymer viscoelasticity *Macromolecules* **51** 3818
[40] Sun Q and Faller R 2006 Systematic coarse-graining of a polymer blend: Polyisoprene and polystyrene *J. Chem. Theor. Comp.* **2** 607
[41] Sun Q and Faller R 2007 Phase separation in polyisoprene/polystyrene blends by a systematically coarse-grained model *J. Chem. Phys.* **126** 144908
[42] Wu C 2013 A combined scheme for systematically coarse-graining of stereoregular polymer blends *Macromolecules* **46** 5751
[43] Wu C 2015 Coarse-grained molecular dynamics simulations of stereoregular poly(methyl methacrylate)/poly(vinyl chloride) blends *J. Polym. Sci.* B **53** 203

[44] Wu C 2016 Phase morphologies of binary polymer blends predicted by systematically coarse-grained models *Macromol. Theory Simul.* **25** 336
[45] Wu C 2020 Transferable coarse-grained models for poly (ethylene oxide)/poly (methyl methacrylate) blends *Comput. Mater. Sci.* **172** 109346
[46] Rudzinski J F 2019 Recent progress towards chemically-specific coarse-grained simulation models with consistent dynamical properties *Computation* **7** 42
[47] Zwanzig R 1960 Ensemble method in the theory of irreversibility *J. Chem. Phys.* **33** 1338
[48] Mori H 1965 Transport, collective mothin and brownian motion *Progr. Theor. Phys.* **33** 424
[49] Kubo R, Toda M and Hashitsumemoto N 2003 *Statistical Physics II: Nonequilibrium Statistical Mechanics* (Berlin: Springer)
[50] Izvekov S and Voth G A 2006 Modeling real dynamics in the coarse-grained representation of condensed phase systems *J. Chem. Phys.* **125** 151101
[51] Hijón C, Espa nol P, Vanden-Eijnden E and Delgado-Buscalioni R 2010 Mori-zwanzig formalism as a practical computational tool *Faraday Discuss* **144** 301
[52] Lyubimov I Y, McCarty J, Clark A and Guenza M G 2010 Analytical rescaling of polymer dynamics from mesoscale simulations *J. Chem. Phys.* **132** 224903
[53] Lyubimov I and Guenza M G 2011 First-principle approach to rescale the dynamics of simulated coarse-grained macromolecular liquids *Phys. Rev.* E **84** 031801
[54] Lyubimov I and Guenza M G 2013 Theoretical reconstruction of realistic dynamics of highly coarse-grained cis-1,4-polybutadiene melts *J. Chem. Phys.* **138** 12A546
[55] Trément S, Schnell B, Petitjean L, Couty M and Rousseau B 2014 Conservative and dissipative force field for simulation of coarse-grained alkane molecules: A bottom-up approach *J. Chem. Phys.* **140** 134113
[56] Deichmann G, Marcon V and van der Vegt. N F A 2014 Bottom-up derivation of conservative and dissipative interactions for coarse-grained molecular liquids with the conditional reversible work method *J. Chem. Phys.* **141** 224109
[57] Kauzlarić D, Meier J T, Espanol P, Greiner A and Succi S 2013 Markovian equations of motion for non-markovian coarse-graining and properties for graphene blobs *New J. Phys.* **15** 125015
[58] Yoshimoto Y, Kinefuchi I, Mima T, Fukushima A, Tokumasu T and Takagi S 2013 Bottom-up construction of interaction models of non-markovian dissipative particle dynamics *Phys. Rev.* E **88** 043305
[59] Zhen Li, Bian X, Caswell B and Karniadakis C E 2014 Construction of dissipative particle dynamics models for complex fluids via the mori-zwanzig formulation *Soft Matter* **10** 8659
[60] Davtyan A, Dama J F, Voth G A and Andersen H C 2015 Dynamic force matching: A method for constructing dynamical coarse-grained models with realistic time dependence *J. Chem. Phys.* **142** 154104
[61] Davtyan A, Voth G A and Andersen H C 2016 Dynamic force matching: Construction of dynamic coarse-grained models with realistic short time dynamics and accurate long time dynamics *J. Chem. Phys.* **145** 224107
[62] Zhen Li, Lee H S, Darve E and Karniadakis G E 2017 Computing the non-markovian coarse-grained interactions derived from the mori-zwanzig formalism in molecular systems: Application to polymer melts *J. Chem. Phys.* **146** 014104
[63] Lemarchand C A, Couty M and Rousseau B 2017 Coarse-grained simulations of cis- and trans-polybutadiene: A bottom-up approach *J. Chem. Phys.* **146** 074904
[64] Yoshimoto Y, Li Z, Kinefuchi I and Karniadakis G E 2017 Construction of non-markovian coarse-grained models employing the mori-zwanzig formalism and iterative boltzmann inversion *J. Chem. Phys.* **147** 244110
[65] Deichmann G and van der Vegt N F A 2018 Bottom-up approach to represent dynamic properties in coarse-grained molecular simulations *J. Chem. Phys.* **149** 244114
[66] Hoogerbrugge P J and Koelman J M V A 1992 Simulating microscopic hydrodynamic phenomena with dissipative particle dynamics *Eur. Phys. Lett.* **19** 155
[67] Espanol P and Warren P 1995 Statistical mechanics of dissipative particle dynamics *Eur. Phys. Lett.* **30** 191
[68] Dquidt A and Canchaya J G S 2015 Bayesian parametrization of coarse-grain dissipative dynamics models *J. Chem. Phys.* **143** 084122
[69] Jose G 2016 Solano Canchaya, Alain Dequidt, Florent Goujon and Patrice Malfreyt. Development of dpd coarse-grained models: From bulk to interfacial properties *J. Chem. Phys.* **145** 054107
[70] Kempfer K, Devemy J, Dequidt A, Couty M and Malfreyt P 2019 Development of coarse-grained models for polymers by trajectory matching *ACS Omega* **4** 3
[71] Prinz J-H *et al* 2011 Markov models of molecular kinetics: generation and validation *J. Chem. Phys.* **134** 174105
[72] Rudzinski J F, Kremer K and Bereau T 2016 Communication: Consistent interpretation of molecular simulation kinetics using markov state models biased with external information *J. Chem. Phys.* **144** 051102
[73] Rudzinski J F and Bereau T 2016 Concurrent parametrization against static and kinetic information leads to more robust coarse-grained force fields *Eur. Phys. J. Special Topics* **225** 1373
[74] Kauzlarić D, Espanol P, Greiner A and Succi S 2011 Three routes to the fricgtion matrix and their application to the coarse-graining of atomic lattices *Macromol. Theory Simul.* **20** 526
[75] Izvekov S 2017 Mori-zwanzig theory for dissipative foces in coarse-grained dynamics in the markov limit *Phys. Rev.* E **95** 013303
[76] Espa nol P, de la Torre J A and Duque-Zumajo D 2019 Solution to the plateau problem in the green-kubo formula *Phys. Rev.* E **99** 022126
[77] Plimpton S J 1995 Fast parallel algorithms for short-range molecular dynamics *J. Comp. Phys.* **117** 1
[78] Abraham M J, Murtola T, Schulz R, Szilard P, Smith J C, Hess B and Lindahl E 2015 Gromacs: High performance molecular simulations through multi-level parallelism from laptops to supercomputers *Software X* **1-2** 19
[79] Halverson J D, Brandes T, Lenz O, Arnold A, Bevc V S S, Kremer K, Stühn T and Reith D 2013 Espresso++: A modern multiscale simulation package for soft matter systems *Comput. Phys. Commun.* **184** 1129
[80] Dünweg B 2003 *Langevin Methods* (Berlin: Springer) p 77
[81] Izvekov A and Voth G A 2005 A multiscale coarse-graining method for biomolecular systems *J. Phys. Chem.* B **109** 2469
[82] Gardiner C 2009 *Stochastic Methods: A Handbook for the Natural and Social Sciences* (Berlin: Springer)
[83] van Kampen N G 2007 *Stochastic Processes in Physics and Chemistry* (Kluwer: North Holland)
[84] Matysiak S, Clementi C, Praprotnik M, Kremer K and Site L D 2007 Modeling diffusive dynamics in adaptive resolution simulation of liquid water *J. Chem. Phys.* **128** 024503
[85] Colmenero J and Arbe A 2007 Segmental dynamics in miscible polymer blends: recent results and open questions *Soft Matter* **3** 1474

[86] Harmandaris V A, Doxastakis M, Mavrantzas V G and Theodorou D N 2002 Detailed molecular dynamics simulation of the self-diffusion of n-alkane and cis-1,4 polyisoprene oligomer melts *J. Chem. Phys.* **116** 436
[87] Doxastakis M, Theodorou D N, Fytas G, Kremer F, Faller R, Müller-Plathe F and Hadjichristidis N 2003 Chain and local dynamics of polyisoprene as probed by experiments and computer simulations *J. Chem. Phys.* **119** 6883
[88] Sharma P, Roy S and Karimi-Varzaneh H A 2016 Validation of force fields of rubber through glass-transition temperature calculation by microsecond atomic-scale molecular dynamics simulation *J. Phys. Chem.* B **120** 1367
[89] Smith G D, Paul W, Monkenbusch M, Willner L, Richter D, Qiu X H and Ediger M D 1999 Molecular dynamics of a 1,4-polybutadiene melt. comparison of experiment and simulation *Macromolecules* **32** 8857
[90] Gestoso P, Nicol E, Doxastakis M and Theodorou D N 2003 Atomistic monte carlo simulation of polybutadiene isomers: cis-1,4-polybutadiene and 1,2-polybutadiene *Macromolecules* **36** 6925
[91] Smith G D and Paul W 1998 United atom force field for molecular dynamics simulations of 1,4-polybutadiene based on quantum chemistry calculations on model molecules *J. Phys. Chem.* A **102** 1200
[92] Nose S 1984 A unified formulation of the constant temperature molecular dynamics methods *J. Chem. Phys.* **81** 511
[93] Hoover W G 1985 *Canonical Dynamics: Equilibrium Phase-Space Distributions* vol 31 p 1695
[94] Parrinello M and Rahman A 1981 Polymorphic transitions in single crystals: A new molecular dynamics method *J. Appl. Phys.* **52** 7182
[95] Auhl D, Ramirez J, Likhtman A E, Chambon P and Fernyhough C 2008 Linear and nonlinear shear flow behavior of monodisperse polyisoprene melts with a large range of molecular weights *J. Rheology* **52** 801
[96] Fetters L J, Lohse D J and Colby R H 2007 *Chain Dimensions and Entanglement Spacings* (New York: Springer) p 447
[97] Carella J M, Graessley W and Fetters L J 1984 Effects of chain microstructure on the viscoelastic properties of linear polymer melts: Polybutadienes and hydrogenated polybutadienes *Macromolecules* **17** 2775
[98] Yi Y X and Zoller P 1993 An experimental and theoretical study of the pvt equation of state of butadiene and isoprene elastomers to 200c to 200mpa *J. Polym. Sci. Part B* **31** 779
[99] Tomlin D W and Roland C M 1992 Negative excess enthalpy in a van der waals polymer mixture *Macromolecules* **25** 2994
[100] Roland C M, Miller J B and McGrath K J 1993 Origin of the negative excess enthalpy in poly(vinylethylene)/cis-l,4-polyisoprene blends *Macromolecules* **26** 4967
[101] Müller M 2010 *Polymer Phase Separation* (Singapore: World Scientific) pp 47
[102] de Gennes P-G 1979 *Scaling Concepts in Polymer Physics* (Ithaca, NY: Cornell University Press)
[103] van der Vegt N F A, Peter C and Kremer K 2008 *Structure-Based Coarse- and Fine-Graining in Soft Matter Simulations* (Boca Raton, FL: CRC Press)
[104] Rühle V, Junghans C, Lukyanov A, Kremer K and Andrienko D 2009 Versatile object-oriented toolkit for coarse-graining applications *J. Chem. Theor. Comp* **5** 3211
[105] Dominik F, Harmandaris V A, Kremer K and van der Vegt N F A 2009 Coarse-grained polymer melts based on isolated atomistic chains: Simulation of polystyrene of different tacticities *Macromolecules* **42** 7579
[106] de Oliveira T E, Netz P A, Kremer K, Junghans C and Mukherji D 2016 C-ibi: Targeting cumulative coordination within an iterative protocol to derive coarse-grained models of (multi-component) complex fluids *J. Chem. Phys.* **144** 174106
[107] Matsuo M and Sasa S ichi 2000 Stochastic energetics of non-uniform temperature systems *Physica* A **276** 188
[108] Doi M and Edwards S F 1986 *The Theory of Polymer Dynamics* (Oxford: Oxford Science)